

Supporting Information

Bioinspired Hybrid Membrane with Wettability and Topology

Anisotropy for High-efficient Fog Collection

Rongjun Hu,^{‡^a,^b} Nü Wang,^{‡^a} Lanlan Hou,^a Zhimin Cui,^a Jingchong Liu,^a Dianming Li,^a Qingzhong Li,^c Hailong Zhang,^b Yong Zhao^{*a}

^a Key Laboratory of Bio-Inspired Smart Interfacial Science and Technology of Ministry of Education, Beijing Key Laboratory of Bioinspired Energy Materials and Devices, School of Chemistry, Beijing Advanced Innovation Center for Biomedical Engineering, Beihang University, Beijing, 100191, P. R. China

E-mail address: zhaoyong@buaa.edu.cn

^b State Key Laboratory for Advanced Metals and Materials, University of Science and Technology Beijing, Beijing, 100083, P. R. China

^c College of Chemistry and Chemical Engineering, Yantai University, Shandong, 264005, P. R. China

‡Rongjun Hu and Nü Wang contributed equally to this work

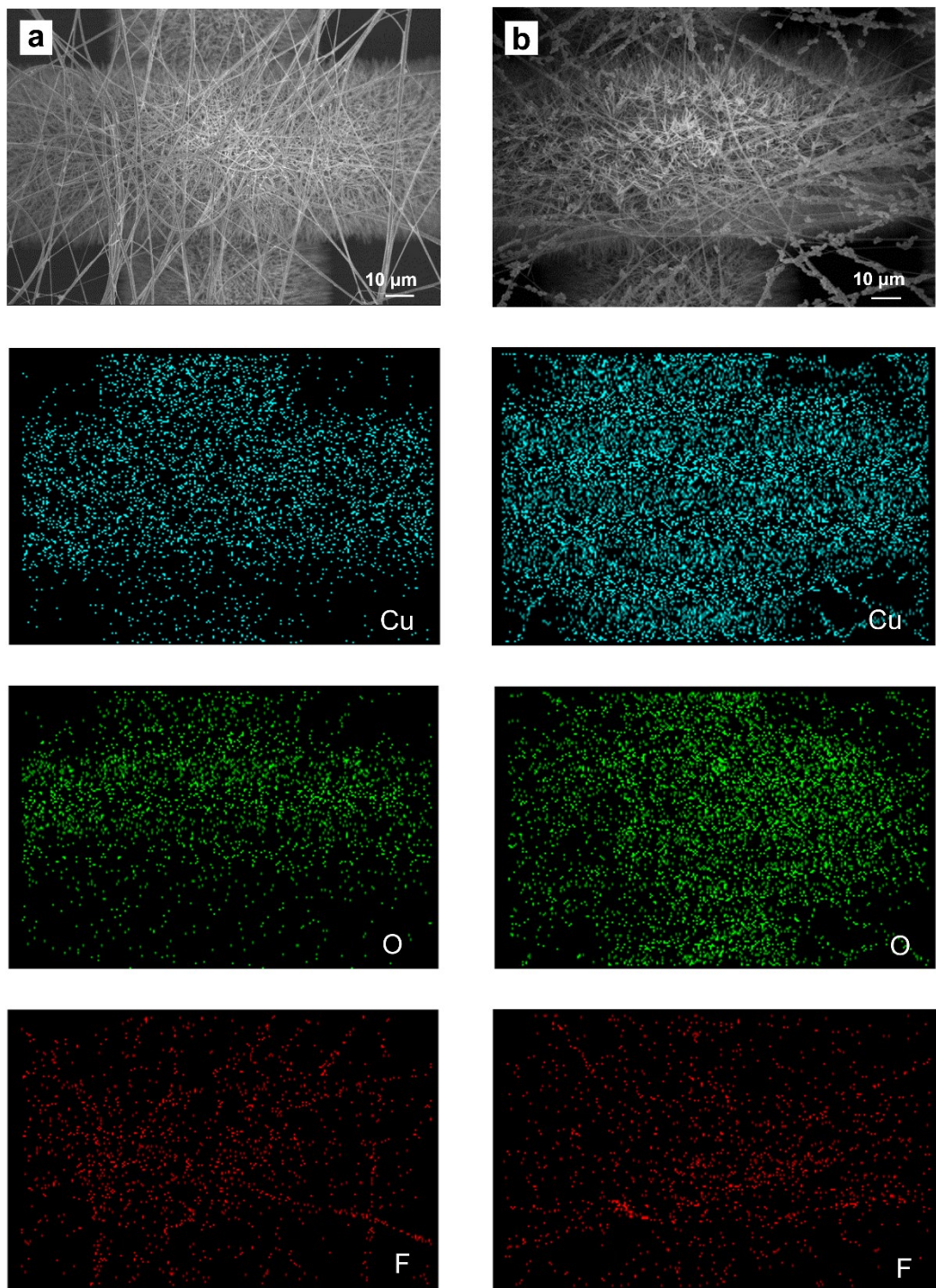


Fig. S1. SEM images via energy dispersive spectroscopy (EDS) analysis on componential elements of the hybrid membrane. For the whole system, Cu-, O-, and F- are indicated with blue, green and red colors, respectively. (Electrospun time is 5 minutes, and anodization time is respectively 600 s, 700 s for a, b).

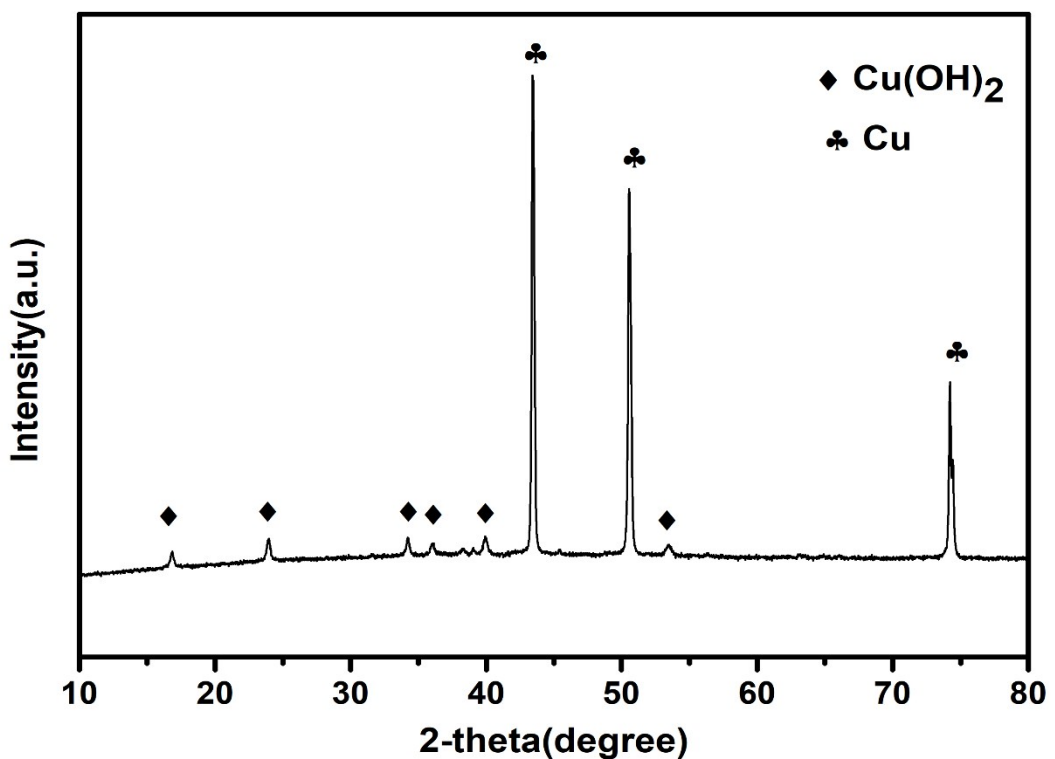


Fig. S2. XRD patterns of Cu mesh after anodization. It demonstrates the Cu changed into the orthorhombic-phase $\text{Cu}(\text{OH})_2$ nanocrystals (JCPDS card no. 13-420).

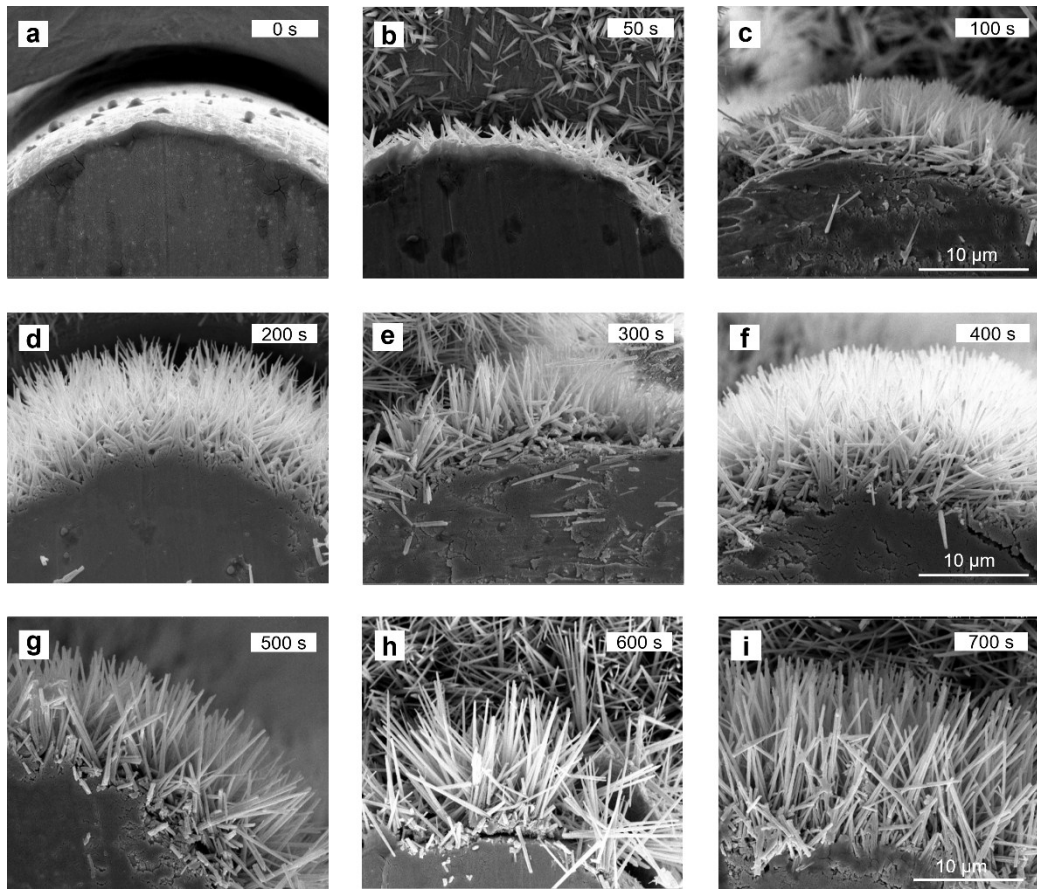


Fig. S3. SEM images of section view of Cu wires with different anodization time: a-i, are respectively anodized 0 s, 50 s, 100 s, 200 s, 300 s, 400 s, 500 s, 600 s and 700 s, for Cu wires. The length of CNNs is linear growth from ~2.2 μm (50 s) to ~12.4 μm (700 s) along with anodization time changed from 50 s to 700 s.

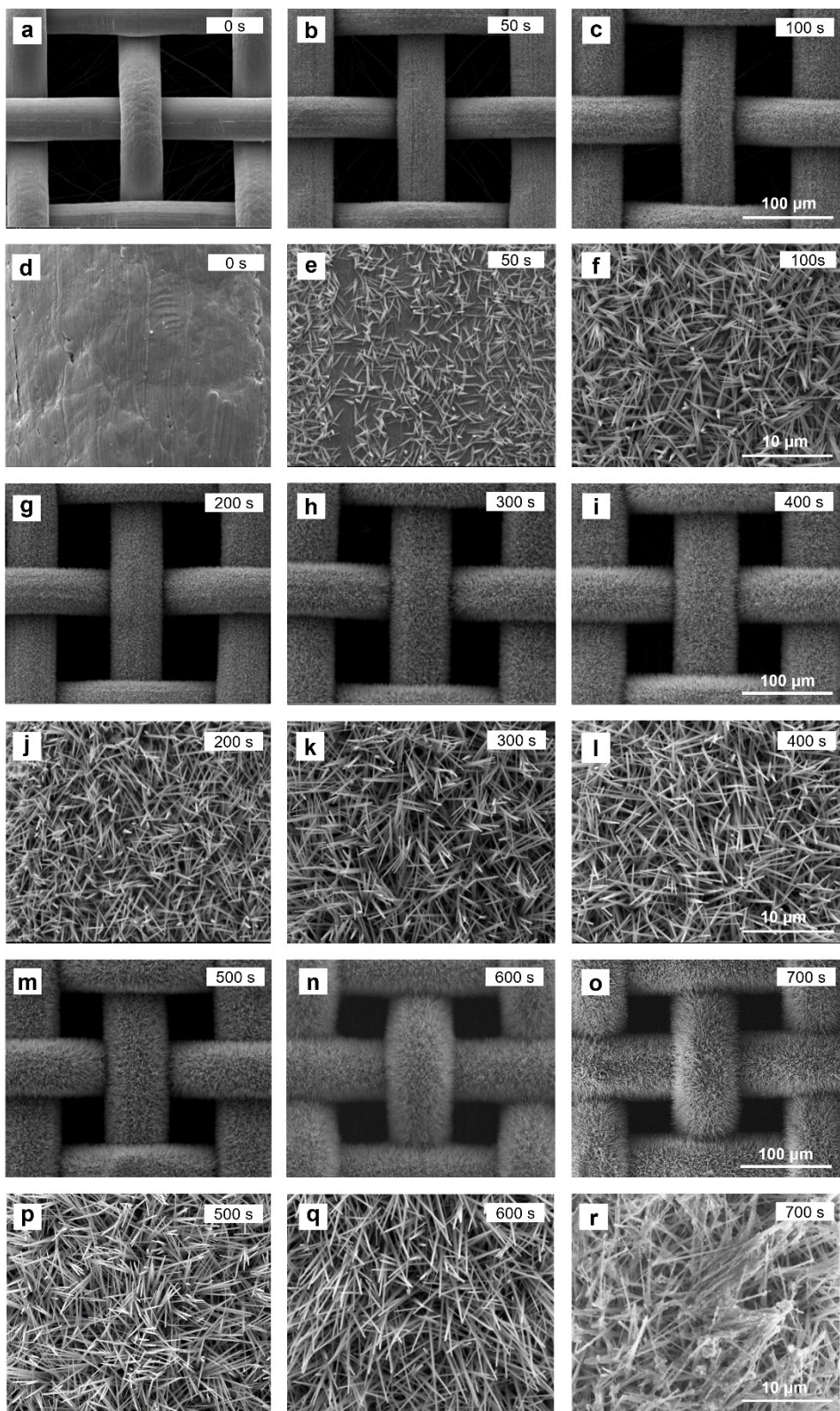


Fig. S4. SEM images of Cu meshes with different anodization time: a-r, are respectively anodized 0 s, 50 s, 100 s, 200 s, 300 s, 400 s, 500 s, 600 s and 700 s, for the Cu mesh. The pore size of anodized Cu meshes decreases from $\sim 75 \mu\text{m}$ to $\sim 50 \mu\text{m}$ with anodization time changed from 0 s to 700 s. The CNNs become inordinate and some conglobate sediments adhere onto the CNNs when anodization time is 700 s.

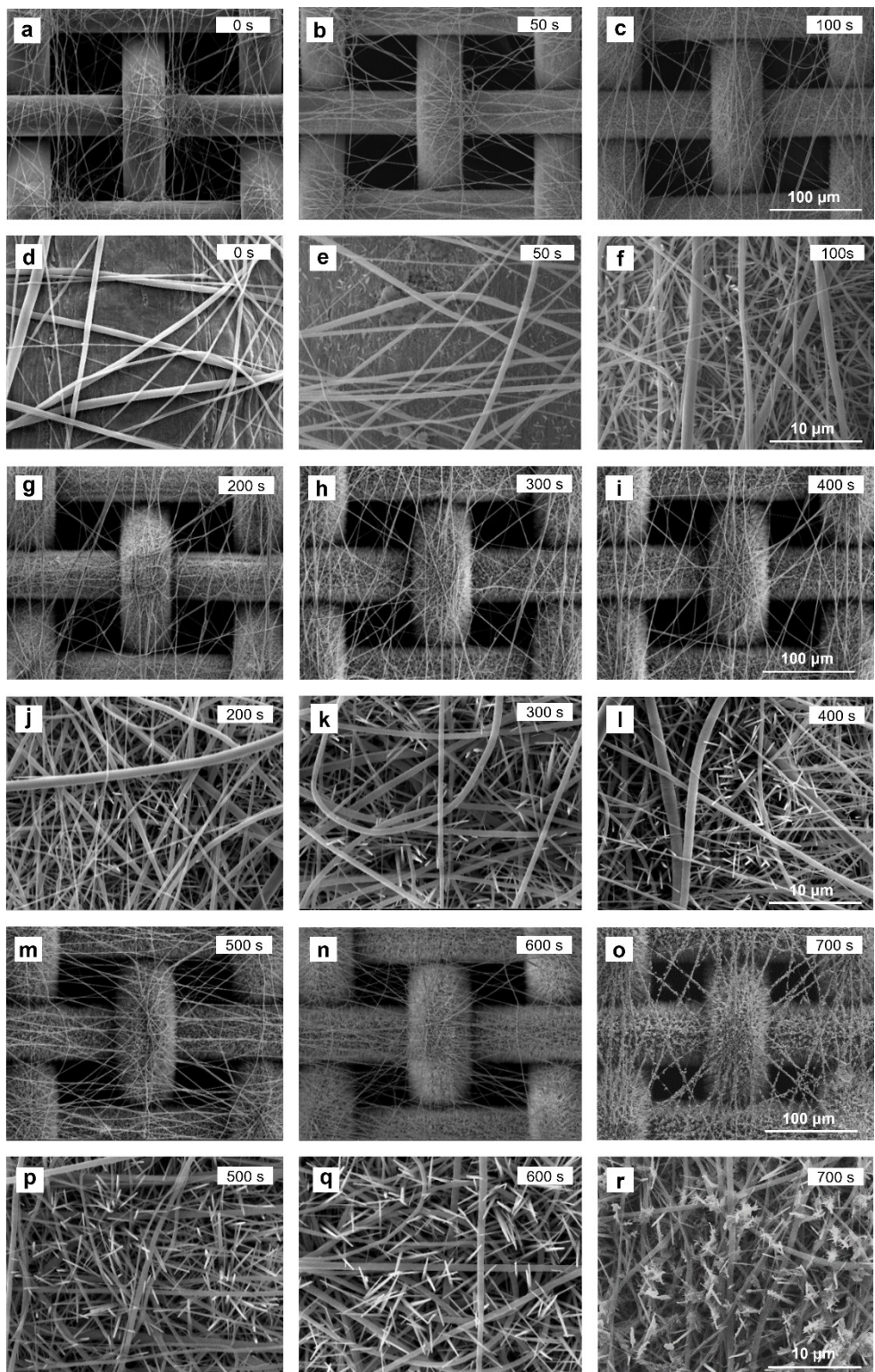


Fig. S5. SEM images of hybrid membrane (electrospun time 5 minutes) with different anodization time: a-r, are respectively anodized 0 s, 50 s, 100 s, 200 s, 300 s, 400 s, 500 s, 600 s and 700 s. The pore size of Cu meshes covered by PNFs network decreases with anodization time changed from 0 to 700 s. The CNNs become inordinate and some conglobate Cu(OH)₂ sediments adhere onto the PNFs and the CNNs when anodization time is 700 s.

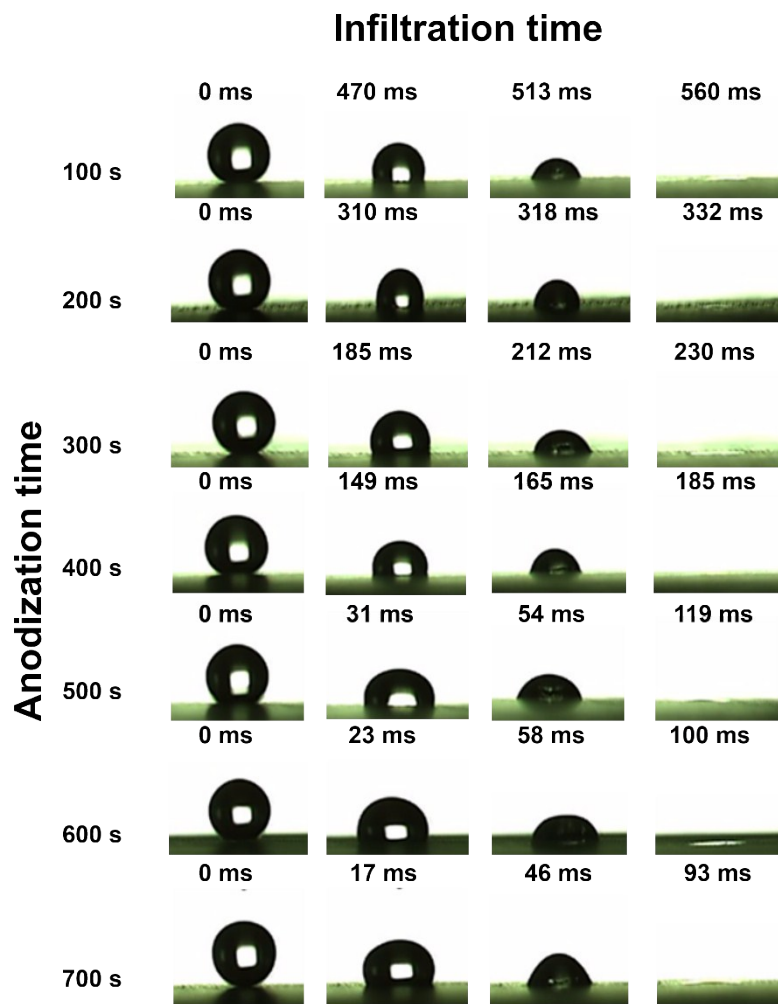


Fig. S6. Optical images of the process which the drops penetrate the hybrid membrane (electrospun time 5 minutes) when anodization time is changed. Infiltration time decreases from 560 ms to 93 ms with anodization time from 100 s to 700 s.

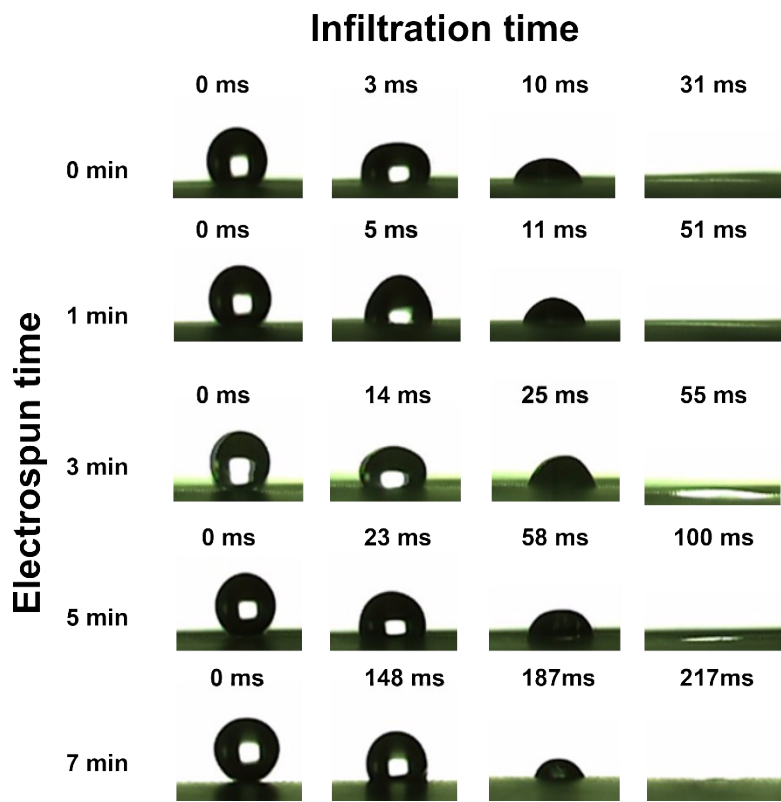


Fig. S7. Optical images of the process which the drops penetrate the hybrid membrane (anodization time 600 s) when electrospun time is changed. Infiltration time increases with electrospun time. Infiltration time increases from 31 ms to 217 ms when electrospun time is from 0 minute to 7 minutes. However, it is noted that the droplet could not permeate the surface if electrospun time is 9 minutes because there are not CNNs piercing the PNFs network.

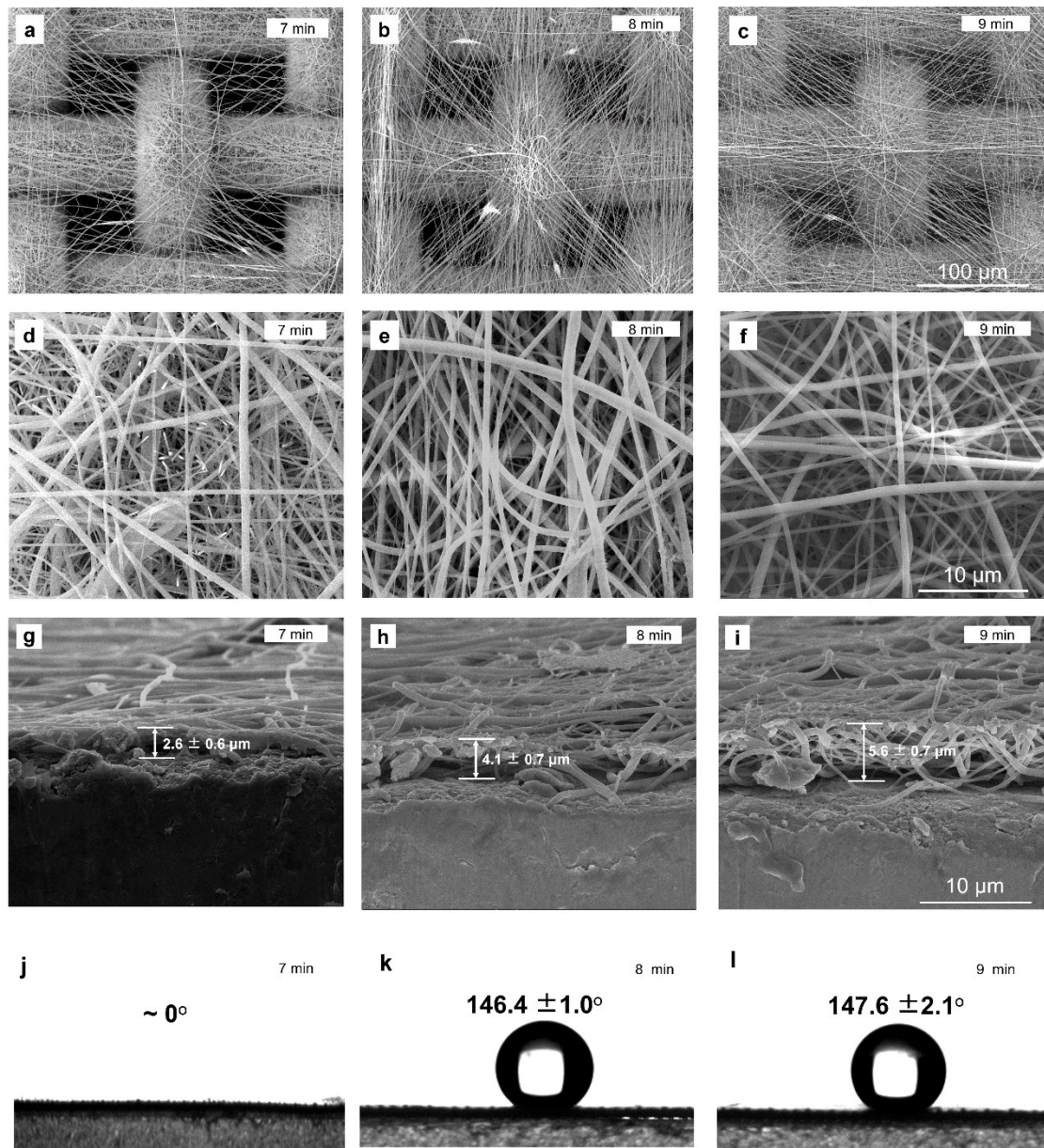


Fig. S8. (a-f) The top view of the hybrid membrane with CNNs/PNFs interleaving topology (anodization time is 600 s, electrospun time is 7, 8, and 9 minutes, respectively.). (g-i) The cross-sectional view of the PNFs. The thickness of the electrospun membrane is about $2.6 \pm 0.6 \mu\text{m}$ (7 min), $4.1 \pm 0.7 \mu\text{m}$ (8 min) and $5.6 \pm 0.7 \mu\text{m}$ (9 min), respectively. (j-l) The contact angles of membranes for electrospun time 7, 8, and 9 minutes, are $\sim 0^\circ$, $146.4 \pm 1.0^\circ$ and $147.6 \pm 2.1^\circ$, respectively.

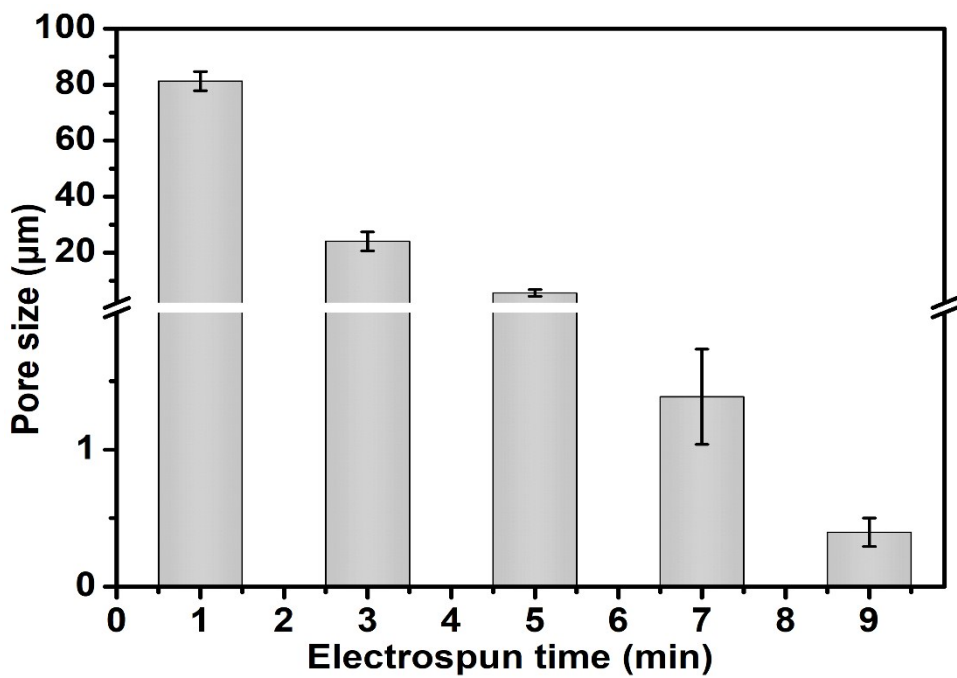


Fig. S9. The relation between pore size of PNFs network and electrospun time. The pore size of fibrous membrane decreases with electrospun time due to the packing effect of PNFs.

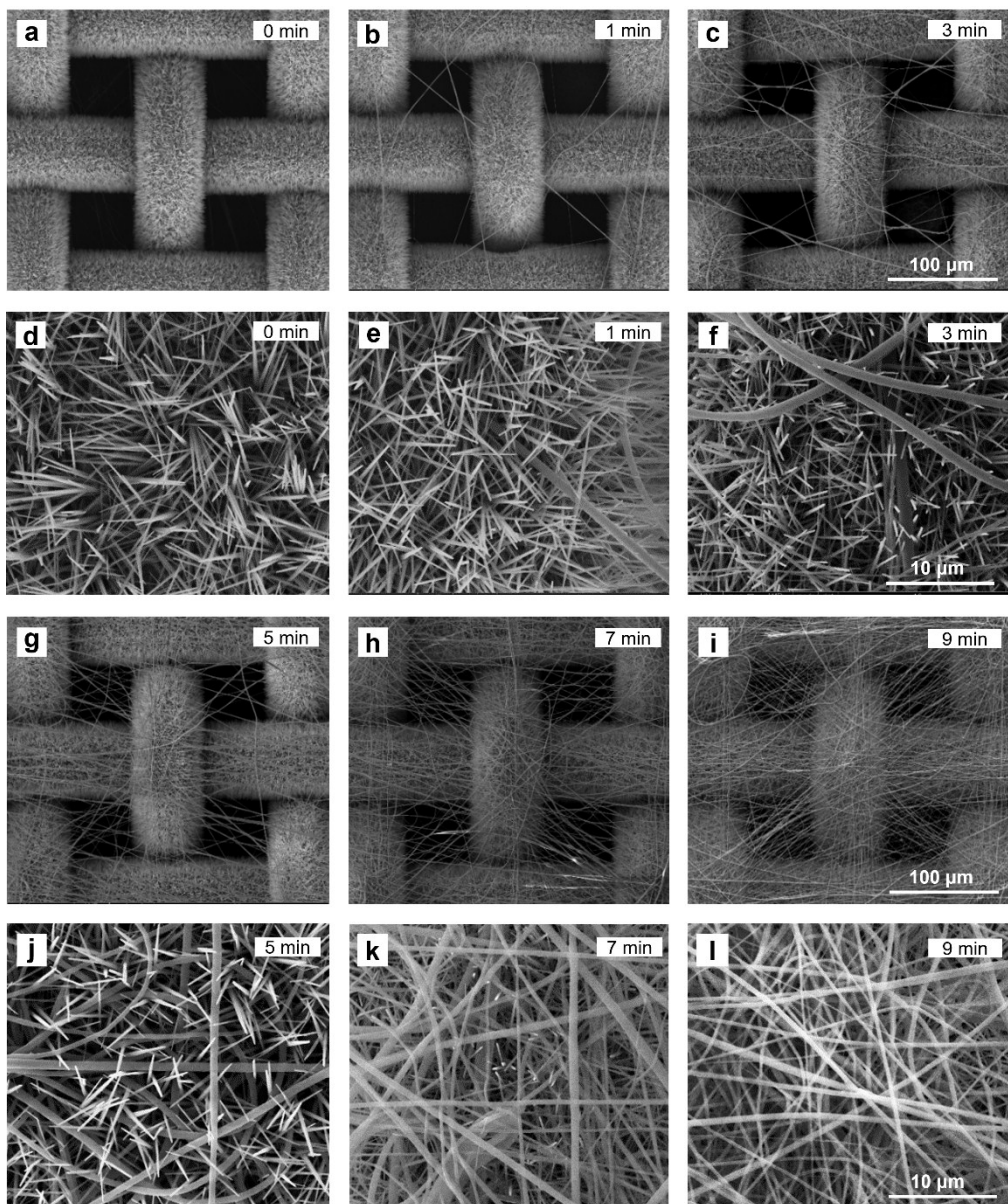


Fig. S10. SEM images of hybrid membrane (anodization time 600 s) with different electrospun time: a-i) electrospun 0, 1, 3, 5, 7 and 9 minutes, respectively. The pore size of fibrous membrane and the length and number of the CNNs above the fibrous membrane decreases with electrospun time. The CNNs is not able to grow out of PNFs network due to very small and winding pores when electrospun time is 9 minutes.

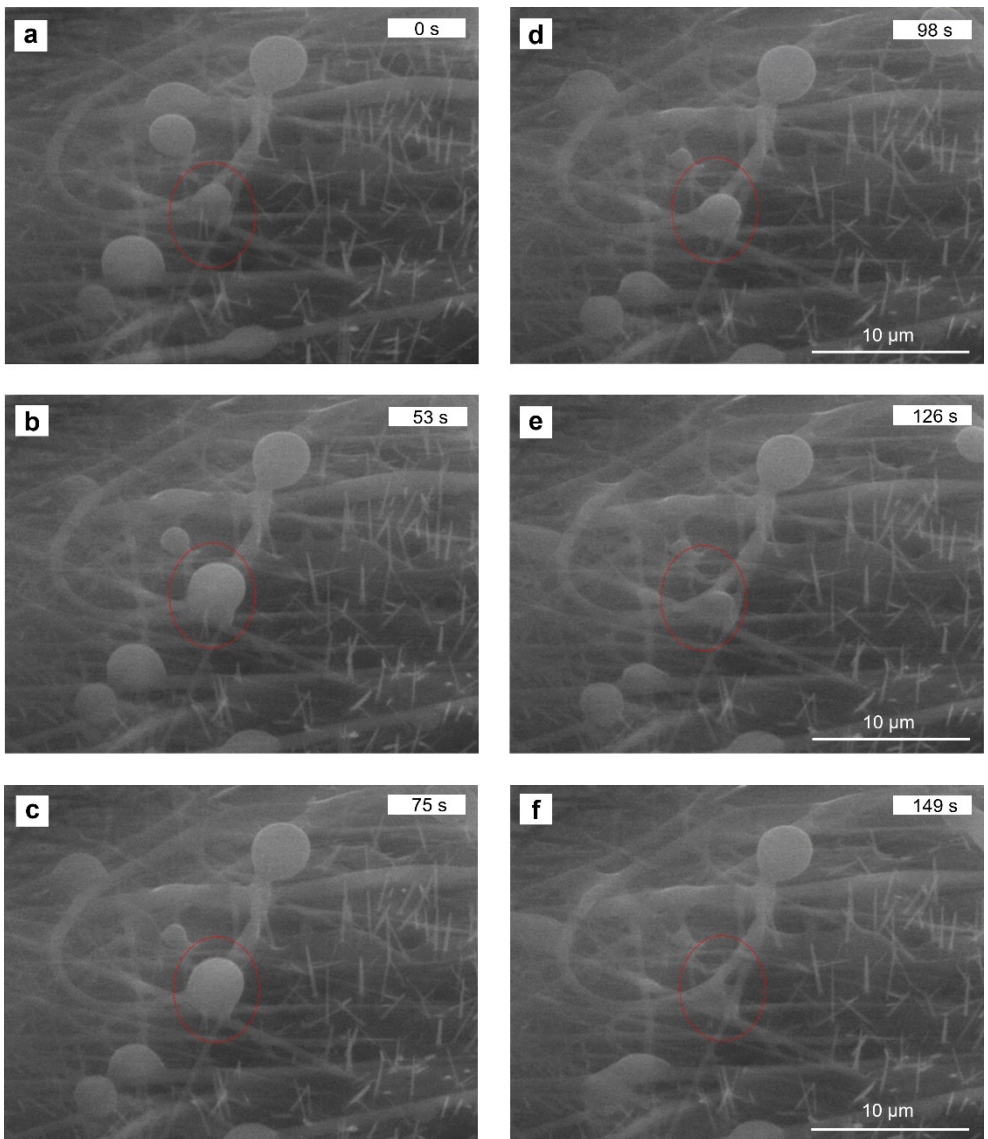


Fig. S11. ESEM images which reveal the droplets condensation and transportation process in the water vapour atmosphere. The droplets are transported away once the droplets only contact the CNNs.

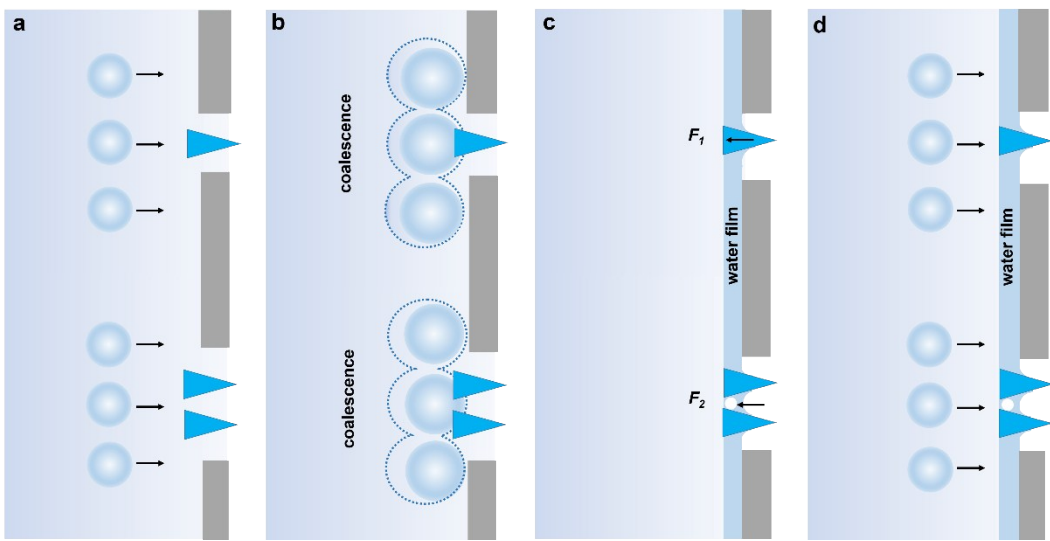


Fig. S12. Proposed model of the spontaneous unidirectional fog transportation for the hybrid membrane when the fog droplets sprays on the CNNs mesh side of the hybrid membrane. The fog droplets cannot be transported from the anodized Cu mesh side to the fibrous membrane side, because of the critical $P_{intrusion}$ and the opposite Laplace force (F_1 and F_2).

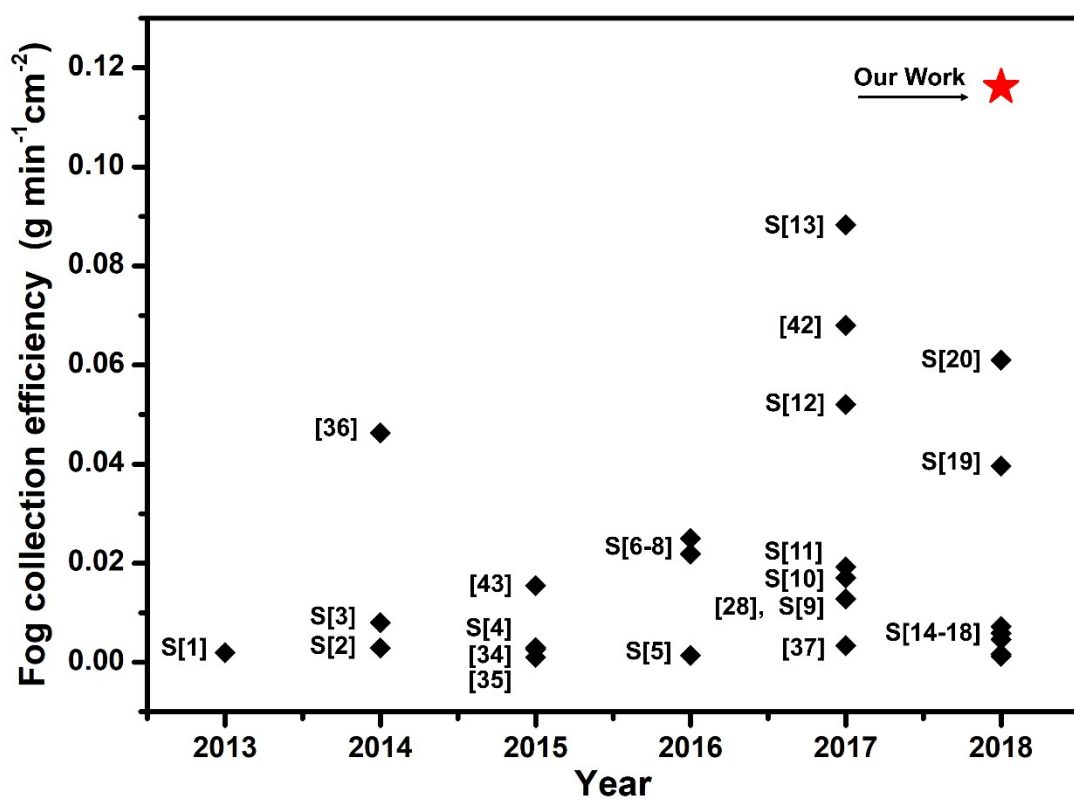


Fig. S13. The fog-collecting efficiency of the hybrid membrane and the results about fog-collecting efficiency for planar materials in recent years. The red star indicates the fog-collecting efficiency of the hybrid membrane which is higher than the other results in recent years. 28, 34-37, 42-43, S1-20

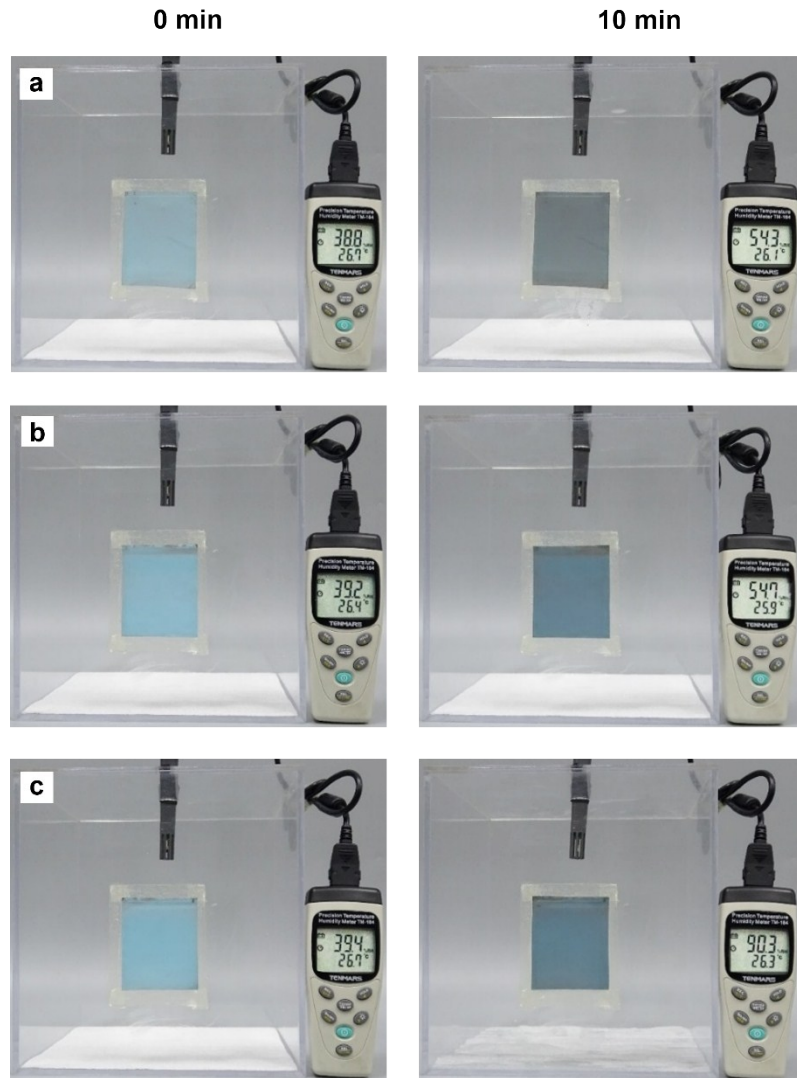


Fig. S14. The humidity change in the chamber when fog drops spray on: (a) the CNNs mesh (without hydrophobic PNFs); (b) the hybrid membrane with hydrophobic PNFs sides inward; (c) the hybrid membrane with hydrophobic PNFs side outward. The humidity changes are respectively, from 38.8% to 54.3%, from 39.2% to 54.7% and 39.4% to 90.3%, after 10 minutes.

References

- S1. B. S. Lalia, S. Anand, K. K. Varanasi and R. Hashaikeh, *Langmuir*, 2013, **29**, 13081-13088.
- S2. S. H. Lee, J. H. Lee, C. W. Park, C. Y. Lee, K. Kim, D. Tahk and M. K. Kwak, *Int. J. Precis. Eng. Manuf-Green Technol.*, 2014, **1**, 119-124.
- S3. C. Liu, J. Ju, Y. Zheng and L. Jiang, *Acs Nano*, 2014, **8**, 1321-1329.
- S4. S. Choo, H. J. Choi and H. Lee, *Appl. Surf. Sci.*, 2015, **324**, 563-568.
- S5. V. A. Ganesh, A. S. Ranganath, A. Baji, H. K. Raut, R. Sahay and S. Ramakrishna, *Macromol. Mater. Eng.*, 2016, **302**, 1600387.
- S6. H. Zhu and Z. Guo, *Chem. Commun.*, 2016, **52**, 6809-6812.
- S7. H. Zhu, F. Yang, J. Li and Z. Guo, *Chem. Commun.*, 2016, **52**, 12415-12417.
- S8. Y. Wang, X. Wang, C. Lai, H. Hu, Y. Kong, B. Fei and J. H. Xin, *ACS Appl. Mater. Interfaces*, 2016, **8**, 2950-2960.
- S9. X. Yang, J. Song, J. Liu, X. Liu and Z. Jin, *Sci. Rep.*, 2017, **7**, 8816.
- S10. N. Thakur, A. S. Ranganath, K. Agarwal and A. Baji, *Macromol. Mater. Eng.*, 2017, **302**, 1700124.
- S11. H. Cho, B. Park, M. Kim, S. Lee and W. Hwang, *J. Mater. Chem. A*, 2017, **5**, 25328.
- S12. M. Wang, Q. Liu, H. Zhang, C. Wang, L. Wang, B. Xiang, Y. Fan, C. Guo and S. Ruan, *ACS Appl. Mater. Interfaces*, 2017, **9**, 29248.
- S13. Z. Yu, F. F. Yun, Y. Wang, L. Yao, S. Dou, K. Liu, L. Jiang and X. Wang, *Small*, 2017,

13, 1701403.

- S14. H. Luo, Y. Lu, S. Yin, S. Huang, J. Song, F. Chen, F. Chen, C. J. Carmalt and I. P. Parkin, *J. Mater. Chem. A*, 2018, **6**, 5635-5643.
- S15. P. Moazzam, H. Tavassoli, A. Razmjou, M. E. Warkiani and M. Asadnia, *Desalination*, 2018, **429**, 111-118.
- S16. V. Sharma, D. Orejon, Y. Takata, V. Krishnan and S. Harish, *ACS Sustainable Chem. Eng.*, 2018, **6**, 6981-6993.
- S17. X. M. Dai, N. Sun, S. O. Nielsen, B. B. Stogin, J. Wang, S. K. Yang and T. S. Wong, *Sci. Adv.*, 2018, **4**, eaaq0919.
- S18. L. S. Zhong, H. Zhu, Y. Wu and Z. G. Guo, *J. Colloid Interface Sci.*, 2018, **525**, 234-242.
- S19. H. Xie, H. X. Huang and H. Y. Mi, *Mater. Lett.*, 2018, **221**, 123-127.
- S20. Y. C. Wu, H. L. Li, L. L. Wen, D. D. Men, L. F. Hang, D. L. Liu, G. Q. Liu, W. P. Cai, X. J. Lyu and Y. Li, *Surf. Innovations*, 2018, **6**, 141-149.